Liping Xie,[1,2] Yue Gu,[2] Mingliang Wen,[2] Shuang Zhao,[2] Wan Wang,[2] Yan Ma,[2] Guoliang Meng,[2] Yi Han,[3] Yuhui Wang,[4] George Liu,[4] Philip K. Moore,[5] Xin Wang,[6] Hong Wang,[7] Zhiren Zhang,[8] Ying Yu,[9] Albert Ferro,[10] Zhengrong Huang,[1] and Yong Ji[2]

Hydrogen Sulfide Induces Keap1 S-sulfhydration and Suppresses Diabetes-Accelerated Atherosclerosis via Nrf2 Activation

Diabetes 2016;65:3171–3184 | DOI: 10.2337/db16-0020

Hydrogen sulfide (H_2S) has been shown to have powerful antioxidative and anti-inflammatory properties that can regulate multiple cardiovascular functions. However, its precise role in diabetes-accelerated atherosclerosis remains unclear. We report here that H_2S reduced aortic atherosclerotic plaque formation with reduction in superoxide (O_2^-) generation and the adhesion molecules in streptozotocin (STZ)-induced $LDLr^{-/-}$ mice but not in $LDLr^{-/-}Nrf2^{-/-}$ mice. In vitro, H_2S inhibited foam cell formation, decreased O_2^- generation, and increased nuclear factor erythroid 2–related factor 2 (Nrf2) nuclear translocation and consequently heme oxygenase 1 (HO-1) expression upregulation in high glucose (HG) plus oxidized LDL (ox-LDL)–treated primary peritoneal macrophages from wild-type but not $Nrf2^{-/-}$ mice. H_2S also decreased O_2^- and adhesion molecule levels and increased Nrf2 nuclear translocation and HO-1 expression, which were suppressed by Nrf2 knockdown in HG/ox-LDL–treated endothelial cells. H_2S increased S-sulfhydration of Keap1, induced Nrf2 dissociation from Keap1, enhanced Nrf2 nuclear translocation, and inhibited O_2^- generation, which were abrogated after Keap1 mutated at Cys151, but not Cys273, in endothelial cells. Collectively, H_2S attenuates diabetes-accelerated atherosclerosis, which may be related to inhibition of oxidative stress via Keap1 sulfhydrylation at Cys151 to activate Nrf2 signaling. This may provide a novel therapeutic target to prevent atherosclerosis in the context of diabetes.

Diabetes leads to a marked increase in atherosclerosis (1). There is considerable evidence demonstrating that oxidative stress and inflammation are involved in the pathogenesis of diabetes and its complications, including atherosclerosis (2). It has been suggested that hyperglycemia-induced superoxide overproduction may be a key event in the activation of pathways involved in the pathogenesis of diabetic complications (2). Approaches that limit oxidative stress may therefore translate to reduced inflammation and hence atherosclerosis.

It is well established that nuclear factor erythroid 2–related factor 2 (Nrf2) is one of the most important cellular defense mechanisms against oxidative stress. Nrf2 is broadly expressed in tissues but is only activated in response to a range of oxidative and electrophilic stimuli (3). Upon

[1]Department of Cardiology, The First Affiliated Hospital of Xiamen University, Xiamen, China
[2]Collaborative Innovation Center for Cardiovascular Disease Translational Medicine, Atherosclerosis Research Centre, Nanjing Medical University, Nanjing, China
[3]Department of Geriatrics, The First Affiliated Hospital of Nanjing Medical University, Nanjing, China
[4]Institute of Cardiovascular Sciences and Key Laboratory of Molecular Cardiovascular Sciences, Ministry of Education, Peking University Health Science Center, Beijing, China
[5]Department of Pharmacology, National University of Singapore, Singapore, Singapore
[6]Faculty of Life Sciences, The University of Manchester, Manchester, U.K.
[7]Center for Metabolic Disease Research, Department of Pharmacology, Temple University School of Medicine, Philadelphia, PA
[8]The Third Affiliated Hospital of Harbin Medical University, Institute of Metabolic Disease, Heilongjiang Academy of Medical Science, Harbin, China
[9]Institute for Nutritional Sciences, Shanghai Institutes for Biological Sciences, Chinese Academy of Sciences, Shanghai, China
[10]Department of Clinical Pharmacology, Cardiovascular Division, British Heart Foundation Centre of Research Excellence, King's College London, London, U.K.

Corresponding authors: Yong Ji, yongji@njmu.edu.cn, and Zhengrong Huang, huangzhengrong@xmu.edu.cn.

Received 11 January 2016 and accepted 15 June 2016.

This article contains Supplementary Data online at http://diabetes.diabetesjournals.org/lookup/suppl/doi:10.2337/db16-0020/-/DC1.

L.X. and Y.G. contributed equally to this work.

See accompanying article, p. 2832.

oxidative stress, Nrf2 escapes Kelch-like ECH-associated protein 1 (Keap1)–mediated repression, translocates to the nucleus, binds to antioxidant response element, and induces the expression of a battery of antioxidant proteins, one of the most important of which is heme oxygenase 1 (HO-1) (4). Nrf2 has emerged as an important target in diabetes and related complications (5,6), and low-dose dh404, which is an analog of the Nrf2 agonist bardoxolone methyl, lowers oxidative stress and protects against diabetes-associated atherosclerosis (7). These studies suggest that augmentation of antioxidant defenses via upregulation of the Nrf2 pathway may be a novel target for the prevention and treatment of diabetic complications.

Hydrogen sulfide (H_2S) plays an important role in physiology and pathophysiology in several biological systems. Emerging data suggest that H_2S improves diabetic endothelial dysfunction (8), nephropathy (9), retinopathy (10), and cardiomyopathy (11). However, there are no published data on the potential effect of H_2S on accelerated atherosclerosis in diabetes.

Some recent studies indicate that H_2S is cytoprotective during myocardial ischemia-reperfusion injury in the setting of diabetes by alleviating oxidative stress, and the ability of H_2S to upregulate cellular antioxidants in the heart in a Nrf2-dependent manner (12–14). H_2S may therefore play an important role in diabetes-accelerated atherosclerosis, and the effects of H_2S may be mediated via activation of Nrf2. In the current study, we have characterized whether and how H_2S targets on Nrf2 against the development of diabetes-accelerated atherosclerosis.

RESEARCH DESIGN AND METHODS

Animals and Treatment

$LDLr^{-/-}$ mice, on a C57BL/6 background, were purchased from the Model Animal Research Center of Nanjing University. $Nrf2^{-/-}$ mice, on a C57BL/6 background, were a gift from Hongliang Li (Renmin Hospital of Wuhan University). $Nrf2^{-/-}$ mice were crossed with $LDLr^{-/-}$ mice to obtain $LDLr^{-/-}Nrf2^{-/-}$. At 8 weeks of age, male mice were rendered diabetic by administering 60 mg/kg/day streptozotocin (STZ) intraperitoneally daily for 5 days. After STZ administration, diabetic mice were administered the H_2S donor GYY4137 (133 μmol/kg/day, i.p.) or vehicle and kept on a high-fat diet (HFD) for 4 weeks. The dose of GYY4137 used was based on previous publications (15). Nondiabetic $LDLr^{-/-}$ or $LDLr^{-/-}Nrf2^{-/-}$ mice were kept on a standard chow diet for 4 weeks as control. Mice were housed (n = 1/cage; n = 6/group) in metabolic cages for 48 h prior to metabolic analysis to acclimate. Body weight, food intake, water intake, and urinary output were determined.

All animal experiments were approved by the Committee on Animal Care of Nanjing Medical University and were conducted according to the National Institutes of Health Guidelines for the Care and Use of Laboratory Animals. All studies involving animals are reported in accordance with the ARRIVE (Animal Research: Reporting of In Vivo Experiments) guidelines.

Blood Sampling

Plasma samples were obtained from mice fasted for 6 h. Glucose was measured directly from the tail tip with a glucometer; plasma lipid levels were measured enzymatically using commercial kits (Zhong Sheng Bei Kong, Peking, China) according to the manufacturer's instructions.

Measurement of Plasma H_2S

Plasma H_2S concentration was measured as described previously (15).

Analysis of Atherosclerotic Lesions

To evaluate atherosclerotic lesions, en face whole and histological sections were used for analysis. The entire aorta attached to the heart was dissected and stained with Oil Red O (ORO; Sigma-Aldrich, St. Louis, MO) (16). Lesions within the sinus were visualized after staining with ORO as well as hematoxylin-eosin (H-E) and quantitated as described previously (16).

Cell Culture and Experimental Conditions

Mouse peritoneal macrophages were isolated from male C57BL/6 or $Nrf2^{-/-}$ mice as described previously (17). Peritoneal cells were collected by lavage and seeded in DMEM–low glucose medium (Gibco, Grand Island, NY) with 10% FBS (Gibco).

Human umbilical vein endothelial cells (HUVECs) were isolated from umbilical cords according to a previously described method (18). The endothelial cells were cultured in Endothelial Cell Medium (ScienCell, Carlsbad, CA).

EA.hy926 endothelial cells were purchased from American Type Culture Collection (Rockville, MD) and were cultured in DMEM–low glucose medium with 10% FBS.

Confluent cells (80–85%) were incubated with D-glucose (25 mmol/L; Sigma-Aldrich) plus oxidized LDL (ox-LDL; 50 mg/L; Yiyuan Biotechnology, Guangzhou, China), in the absence or presence of GYY4137 (50 or 100 μmol/L), sulfide-depleted GYY4137 (SDG; dissolved GYY4137 left unstoppered at room temperature for 5 days), or ZYJ1122 (a structural analog of GYY4137 lacking sulfur) for 24 h.

Small Interfering RNA or Plasmid Transfection

EA.hy926 cells were transfected with small interfering RNA (siRNA) oligonucleotide against Nrf2 (sense: 5′AAG AGUAUGAGCUGGAAAAACdTdT-3′, antisense: 5′GUUUU UCCAGCUCAUACAUUCdTdT-3′; Genepharma) or negative control siRNA. HO-1 expression was silenced by HO-1 siRNA mix that was purchased from Santa Cruz Biotechnology. The plasmid pcDNA3-flag-Keap1 purchased from Addgene (Cambridge, MA) was termed as Keap1-WT. Single mutation at Cys151, -273, or -288 to Ala (Haibio, Shanghai, China) was confirmed by DNA sequencing. EA.hy926 cells were transfected with expression vectors using the Lipofectamine 3000 reagent (Invitrogen).

Foam Cell Formation Assay

Macrophages were fixed with 4% paraformaldehyde and stained using 0.5% ORO. Images of cells were acquired using a light microscope (Nikon, Tokyo, Japan).

Measurement of Reactive Oxygen Species Formation

Superoxide production in tissue sections of upper descending thoracic aorta and cells was detected by dihydroethidium (DHE) assay according to the manufacturer's instructions. In brief, cells or tissue were incubated with DHE for 30 min. Fluorescence was measured with a Nikon TE2000 inverted microscope and quantified using Image-Pro Plus analysis software.

Immunofluorescence Staining

Sections or cells were fixed and permeabilized and then blocked and incubated with antibody against Nrf2, vascular cell adhesion molecule-1 (VCAM-1), intercellular adhesion molecule-1 (ICAM-1), CD31, α-SMA, or macrophage (Abcam, Cambridge, MA). After additional washing, sections or cells were incubated with directly conjugated fluorescent secondary antibodies and DAPI (Invitrogen). Fluorescence was imaged using a Nikon TE2000 inverted microscope. Positive cells and total cells were quantified in five different sections from six different mice of each genotype, using Image-Pro Plus analysis software.

RNA Analysis

HO-1, ICAM-1, VCAM-1, thioredoxin (Trx), and glutamate cysteine ligase catalytic subunit (GCLC) mRNA expression was quantified by real-time PCR (RT-PCR) with forward and reverse primers (Supplementary Table 1).

Isolation of Nuclear and Cytoplasmic Proteins and Western Blotting

Whole-cell, cytosolic, and nuclear proteins were extracted using RIPA buffer (Sigma-Aldrich) or a nuclear and cytoplasmic extraction kit (Thermo Fisher Scientific). Western blotting was performed as described previously (19). Primary antibodies included anti-Nrf2 (Santa Cruz Biotechnology, CA), anti-Nrf2 (phospho S40; Abcam), anti–HO-1 (Bioworld Technology Inc., Nanjing, China), anti–VCAM-1 (Abcam), anti–ICAM-1 (Abcam), anti–histone H3 (Bioworld Technology, Inc.), and anti-GAPDH (Abcam). Band intensities were analyzed using ImageJ 1.25 software.

Immunoprecipitation

The cells were harvested and lysed as previously described (20). Antibodies specific to Keap1 (Santa Cruz Biotechnology) or normal rabbit IgG were added to the supernatants followed by an incubation. Immune complexes were then precipitated with protein A agarose beads. Bound proteins were eluted by boiling with loading buffer and analyzed by Western blotting with anti-Nrf2 antibody.

"Tag-Switch" Method

Nrf2 and Keap1 S-sulfhydration was detected with the "tag-switch" method (21). The protein of Keap1 was pulled down with immunoprecipitation and treated with biotin-linked cyanoacetate. Samples were resuspended in Laemmli buffer, heated, and subjected to Western blotting analysis using anti-biotin antibody (Santa Cruz Biotechnology).

Statistical Analysis

Data are expressed as mean ± SEM and were analyzed by one-way ANOVA followed by Newman-Keuls multiple comparison test as appropriate. All statistical analyses were performed using SPSS software, version 16.0. A value of $P < 0.05$ was considered statistically significant.

RESULTS

Metabolic Characteristics and Plasma Level of H_2S

As expected, diabetic LDL$r^{-/-}$ mice fed an HFD had lower body weight, higher plasma total cholesterol, triacylglycerol, urinary output, water intake, and food intake when compared with those fed standard chow, and these effects were unaffected by treatment with GYY4137 (Supplementary Table 2). Compared with LDL$r^{-/-}$ mice, plasma H_2S concentration was reduced in HFD-fed diabetic LDL$r^{-/-}$ mice, which could be significantly increased by administration of GYY4137 (Supplementary Table 2).

H_2S Decreases Atherosclerotic Lesions in Diabetic LDL$r^{-/-}$ Mice

To determine the effect of H_2S on the formation of atherosclerotic lesions in STZ-diabetic LDL$r^{-/-}$ mice, these animals were treated with GYY4137 or vehicle for 4 weeks, and an HFD was used to enhance atherogenesis (Fig. 1*A*). Initially, we measured the total aortic lesion area between the proximal ascending aorta and the bifurcation of the iliac artery by en face analysis of ORO-stained aortas. As expected, diabetic mice showed an increase in atherosclerotic plaques compared with the nondiabetic control. Treatment of diabetic LDL$r^{-/-}$ mice with H_2S reduced lesion area (Fig. 1*B* and Supplementary Fig. 1). Similar results were confirmed by H-E and ORO staining in the aortic root (Fig. 1*C* and *D*). Immunofluorescence analysis of sections from the aortic root revealed that macrophage content was increased in diabetic LDL$r^{-/-}$ mice, and this effect was attenuated by H_2S treatment (Fig. 1*E* and *F*). Collectively, these data demonstrate that exogenous H_2S decreases atherosclerotic lesions in diabetic LDL$r^{-/-}$ mice.

H_2S Reduces the Level of Superoxide, VCAM-1, and ICAM-1 and Activates Expression of Nrf2 and Associated Antioxidant Proteins in Vessels of Diabetic LDL$r^{-/-}$ Mice

Oxidative stress plays an important role in the pathogenesis of diabetes and its complications. To determine whether the protective role of H_2S in atherosclerotic lesions might relate to reduction of reactive oxygen species (ROS), we measured aortic superoxide formation by DHE assay. As expected, compared with nondiabetic LDL$r^{-/-}$ mice, endothelial fluorescence was increased in diabetic LDL$r^{-/-}$ mice. In contrast, endothelial superoxide production in diabetic LDL$r^{-/-}$ mice was attenuated after GYY4137 administration (Fig. 2*A* and *B*). Several recent studies have identified Nrf2 as a critical transcription factor that regulates a battery of antioxidant genes in the face of oxidative stress (3). Recent work has also shown that H_2S regulates Nrf2 in myocardial tissue (12). To examine

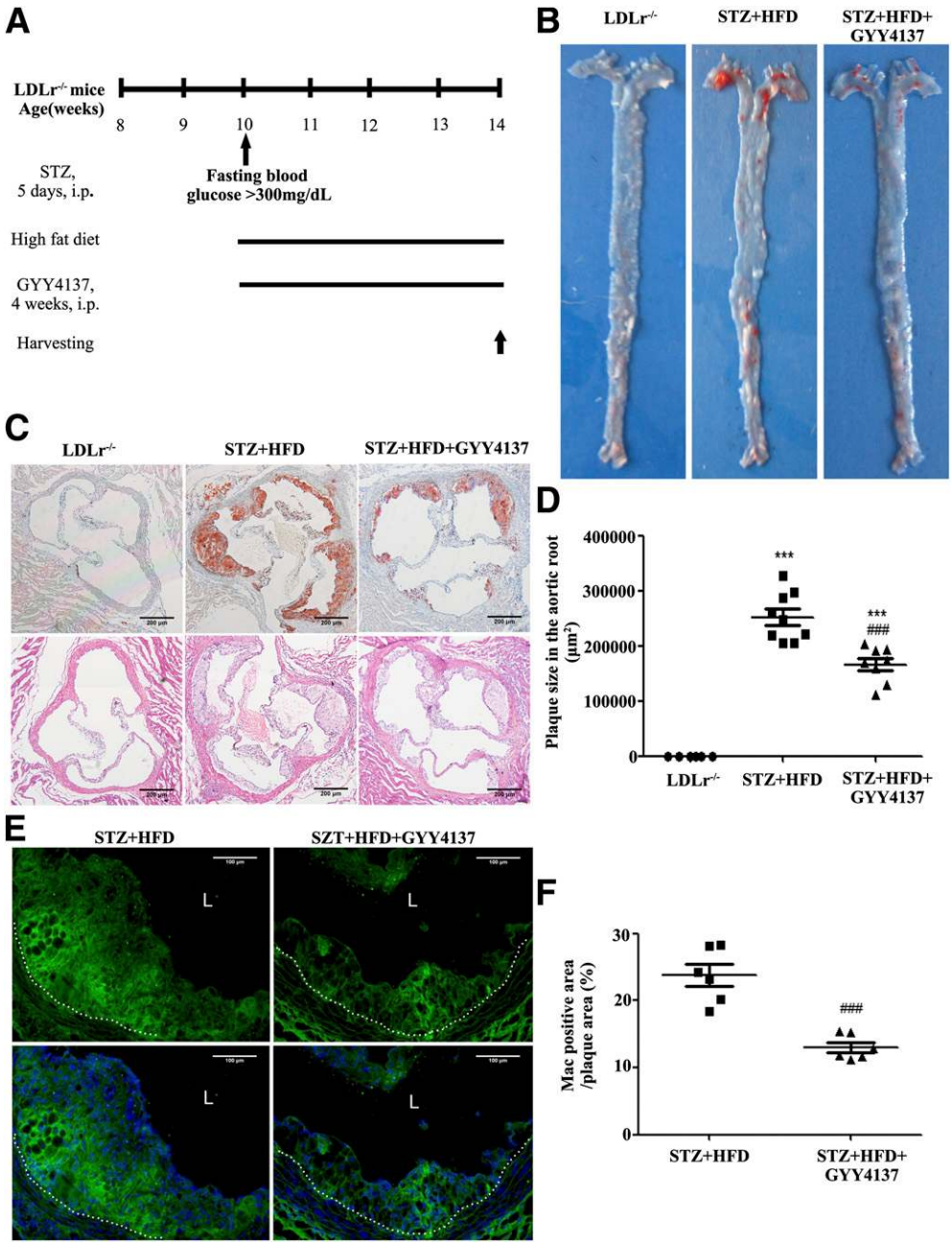

Figure 1—Effects of H_2S on atherosclerosis in HFD-fed diabetic LDLr$^{-/-}$ mice. Diabetic LDLr$^{-/-}$ mice were fed an HFD and received daily intraperitoneal injection of saline or H_2S donor GYY4137 (133 μmol/kg/day) for 4 weeks. *A*: Schema of experimental procedure. *B*: Lesion areas shown were quantified using ORO staining of the thoracoabdominal aorta. *C* and *D*: Representative ORO- and H-E–stained images and quantification of aortic sinus sections from LDLr$^{-/-}$ (n = 6), STZ+HFD (n = 9), and STZ+HFD+GYY4137 (n = 8) mice. Scale bars, 200 μm. *E* and *F*: Frozen sections of aortic root were stained for antimacrophage (green) and DAPI (blue). Dotted lines indicate the boundary of lesion and aortic tunica intima. Quantitative data in the graph represent the positively stained area percentage of plaque (n = 6). Scale bars, 100 μm. Data shown are mean ± SEM. ***P < 0.001 vs. LDLr$^{-/-}$ mice; ###P < 0.001 vs. STZ+HFD mice. L, lumen.

whether Nrf2 is activated in response to H_2S treatment, we investigated the intracellular localization of Nrf2. Immunofluorescence microscopy showed enhanced nuclear staining of Nrf2 in aortas of H_2S-treated in comparison with untreated diabetic LDLr$^{-/-}$ mice (Fig. 2*C*). To further confirm the Nrf2 localization, we performed double staining for Nrf2 and CD31 (endothelial marker), α-SMA (smooth muscle cells marker), or macrophage marker and found that Nrf2 could be clearly shown colocalized with three markers in aorta. Also, GYY4137 treatment increased Nrf2 nuclear translocation in aortic endothelial cells, smooth muscle cells, and macrophages (Supplementary Fig. 2). In addition, the induction of expression of the Nrf2-related antioxidant defense enzyme HO-1 was substantially increased by H_2S (Fig. 2*D*); whereas other Nrf2 target genes, such as Trx and GCLC, were unchanged (Supplementary Fig. 3).

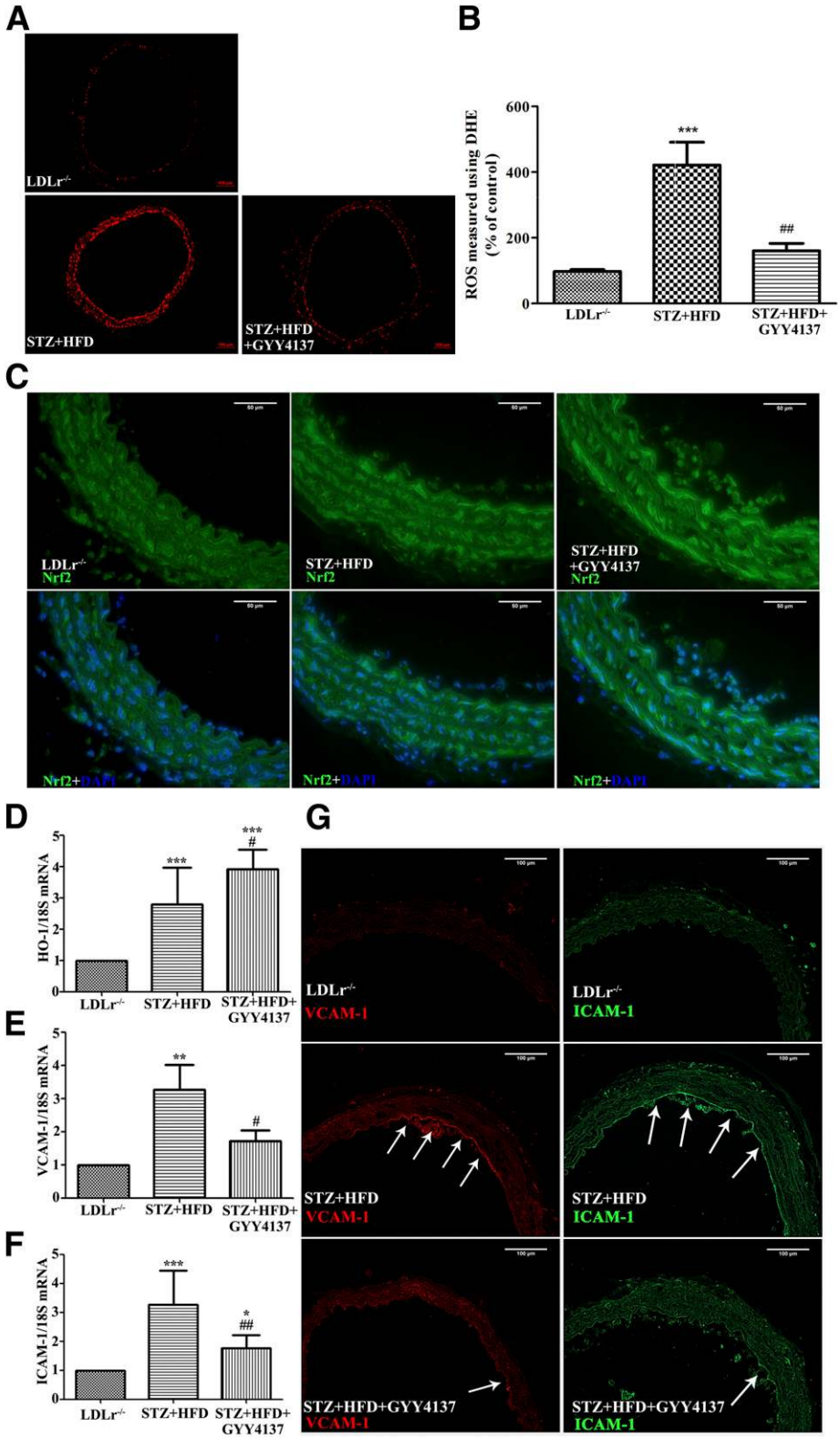

Figure 2—Effects of H_2S on ROS formation and Nrf2, VCAM-1, and ICAM-1 expression in aortas from HFD-fed diabetic LDLr$^{-/-}$ mice. *A*: Representative DHE fluorescence image of aortic tissue from LDLr$^{-/-}$, STZ+HFD, and STZ+HFD+GYY4137 mice. Scale bars, 100 μm. *B*: Quantification of DHE fluorescence image of *A*. ***P < 0.001 vs. LDLr$^{-/-}$ mice; ##P < 0.01 vs. STZ+HFD mice. n = 6. *C*: Representative immunostaining for Nrf2 (green) and DAPI (blue) of aorta. Scale bars, 50 μm. *D*: mRNA levels of HO-1 in the aortas of LDLr$^{-/-}$ (n = 6), STZ+HFD (n = 6), and STZ+HFD+GYY4137 (n = 8) mice, as determined by quantitative RT-PCR analysis. mRNA levels of VCAM-1 (*E*) and ICAM-1 (*F*) in the aortas of LDLr$^{-/-}$ (n = 6), STZ+HFD (n = 6), and STZ+HFD+GYY4137 (n = 6) mice. *G*: Representative VCAM-1 and ICAM-1 immunostaining of aortic arch section (with arrows). Scale bars, 100 μm. *P < 0.05, **P < 0.01, and ***P < 0.001 vs. LDLr$^{-/-}$ mice; #P < 0.05 and ##P < 0.01 vs. STZ+HFD mice.

Oxidative stress induces the expression of adhesion molecules such as VCAM-1 and ICAM-1, which promote the recruitment to, and accumulation of, inflammatory cells within the developing atherosclerotic lesion. Therefore, the levels of VCAM-1 and ICAM-1 in aorta were determined by RT-PCR and immunofluorescence. After 4 weeks on HFD, both VCAM-1 and ICAM-1 increased in diabetic $LDLr^{-/-}$ mice, and this effect was abrogated by treatment with H_2S (Fig. 2*E*–*G* and Supplementary Fig. 4). Together, these results indicate that exogenous H_2S attenuates diabetes-accelerated atherosclerosis, most likely by maintaining redox balance via the Nrf2 pathway.

Nrf2 Deficiency Abolishes the Protective Effects of H_2S in STZ-Induced $LDLr^{-/-}$ Mice

To further explore the pathophysiological significance of H_2S-induced Nrf2 activation in vivo, we mated $LDLr^{-/-}$ mice with $Nrf2^{-/-}$ mice to generate $LDLr^{-/-}Nrf2^{-/-}$ mice. After injection of STZ and 4 weeks of HFD, with or without concomitant GYY4137 treatment, metabolic characteristics were assessed (Supplementary Table 3). Histological assessment of atherosclerotic lesions at the aortic sinus by ORO and H-E staining showed a marked increase of plaques in the aortic root from $LDLr^{-/-}Nrf2^{-/-}$ diabetic mice fed HFD, and the aortic plaque area was now not reduced by H_2S treatment (Fig. 3*A* and *B*). Moreover, the expressions of superoxide, VCAM-1, and ICAM-1 were not reduced after treatment of GYY4137 in diabetic $LDLr^{-/-}Nrf2^{-/-}$ mice (Fig. 3*C*–*G* and Supplementary Fig. 5). Complementary analyses of Nrf2 target gene levels in aorta revealed that the expression of HO-1 could not be augmented by H_2S in the presence of Nrf2 deficiency (Fig. 3*H*). These results demonstrate that Nrf2 is necessary for the inhibitory effect of H_2S to be exerted on diabetes-accelerated atherosclerosis in vivo.

H_2S Decreases Foam Cell Formation and Production of Superoxide and Enhances HO-1 Expression via Activation of Nrf2 in High Glucose Plus ox-LDL–Treated Mouse Macrophages

Accumulation of cholesterol and cholesteryl esters in macrophages and subsequent foam cell formation is a critical early event in atherogenesis. To further investigate the molecular mechanisms underlying the effects of H_2S, we established a macrophage model in hyperglycemic and hyperlipidemic conditions in vitro, which replicates some of the characteristics of macrophages in the diabetes-accelerated atherosclerotic mouse model. Mouse peritoneal macrophages from C57BL/6 were incubated with high glucose (HG) plus ox-LDL (HG+ox-LDL), with or without GYY4137 for 24 h, after which foam cell formation and ROS production were measured by ORO staining and DHE assay, respectively. As expected, foam cell formation was induced in macrophages exposed to ox-LDL, and this effect was exaggerated by coincubation with HG (data not shown). Pretreatment with GYY4137 (50 or 100 μmol/L), but not SDG or ZYJ1122, abrogated this effect (Fig. 4*A* and Supplementary Fig. 6). In addition, superoxide generation was enhanced in HG+ox-LDL–stimulated macrophages (Fig. 4*B* and *C*), and this too was attenuated by pretreatment with H_2S.

Next, to test whether Nrf2 is involved in the effects of H_2S on macrophage function, we investigated its intracellular localization. Immunofluorescence microscopy showed enhanced nuclear staining of Nrf2 in cells treated with H_2S in comparison with vehicle-treated cells, in the presence of HG+ox-LDL (Fig. 4*D*). Western blotting analysis of cytoplasmic and nuclear protein extracts also indicated increased nuclear accumulation of Nrf2 protein in cells treated with H_2S (Fig. 4*E* and *F*), suggesting that Nrf2 is activated in response to H_2S exposure. Similarly, in the presence of HG+ox-LDL, H_2S-pretreated macrophages exhibited increased production of HO-1 (Fig. 4*G*).

Additional experiments were performed to confirm the involvement of Nrf2 in the protective effect of H_2S, using mouse peritoneal macrophages isolated from $Nrf2^{-/-}$ mice. Inhibition of foam cell formation and superoxide generation induced by HG+ox-LDL was attenuated by H_2S treatment in Nrf2 knockout (KO) cells (Fig. 5*A*–*C*). Consistent with these results, elevation of HO-1 expression by H_2S treatment was also abolished in the Nrf2 KO group (Fig. 5*D*). Furthermore, HO-1 knockdown by siRNA or inhibition by ZnPP (HO-1 inhibitor) also abrogated H_2S-mediated suppression of O_2^- generation and foam cell formation (Supplementary Fig. 7). These results demonstrate that the Nrf2/HO-1 pathway is responsible for the inhibitory effects of H_2S on HG+ox-LDL–induced foam cell formation and oxidative stress in macrophages.

H_2S Decreases ROS, ICAM-1, and VCAM-1 Generation and Enhances HO-1 Expression via Nrf2 Signaling in HG+ox-LDL–Treated Endothelial Cells

It has been reported that endothelial dysfunction caused by lipotoxicity or hyperglycemia is mediated through several mechanisms, including increased oxidative stress and proinflammatory responses. Therefore, we measured the effect of H_2S on oxidative stress in endothelial cells by DHE assay. Stimulation of HUVECs with HG+ox-LDL for 24 h caused an increase in the production of superoxide, and this increase was alleviated by pretreatment with GYY4137 (50 or 100 μmol/L) (Fig. 6*A* and *B*) but not with SDG or ZYJ1122 (Supplementary Fig. 8).

To confirm whether the cytoprotective effect of H_2S against oxidative stress was also associated with Nrf2, we carried out immunofluorescence and Western blotting for Nrf2. GYY4137 had no effect on Nrf2 phosphorylation, but can increase the Nrf2 protein expression in the nuclear in HG+ox-LDL–stimulated endothelial cells (Fig. 6*C*–*E* and Supplementary Fig. 9A), implying that H_2S may promote phosphorylation-independent Nrf2 nuclear translocation. Consistent with our in vivo study, H_2S reduced the expression of VCAM-1 and ICAM-1 (Fig. 6*F* and *G*); in addition, the Nrf2 target gene HO-1 was also increased by H_2S pretreatment (Fig. 6*H* and *I*). To further clarify whether H_2S-induced downregulation of oxidative stress was dependent

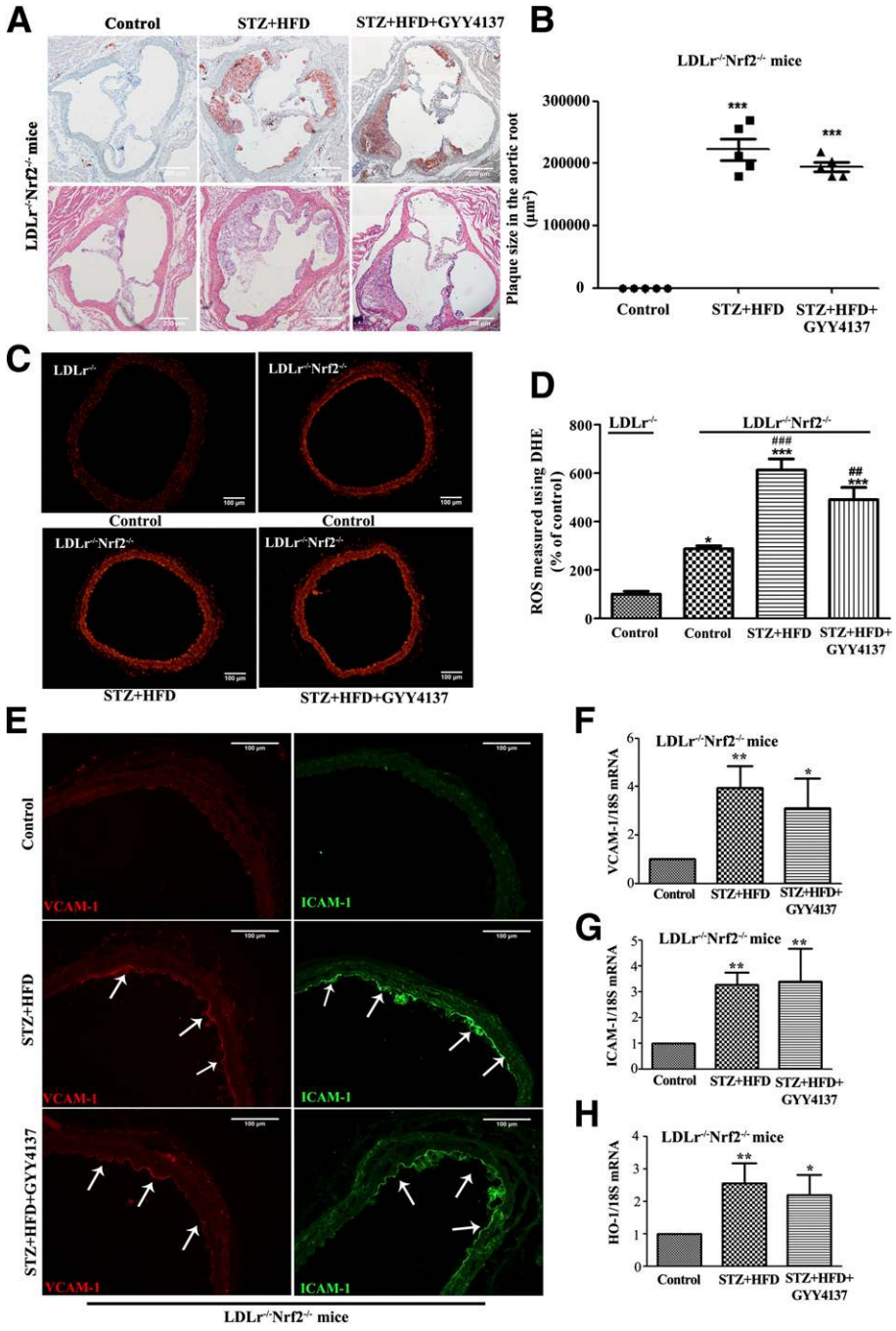

Figure 3—Effects of H_2S on diabetes-accelerated atherosclerosis in LDLr$^{-/-}$Nrf2$^{-/-}$ mice. Diabetic LDLr$^{-/-}$Nrf2$^{-/-}$ mice were fed an HFD and received daily intraperitoneal injection of saline or GYY4137 (133 μmol/kg/day) for 4 weeks. *A* and *B*: Representative ORO- and H-E–stained images and quantification of aortic sinus sections from LDLr$^{-/-}$Nrf2$^{-/-}$, STZ+HFD, and STZ+HFD+GYY4137 mice (n = 5). Scale bars, 200 μm. *C*: Representative DHE fluorescence image of aorta. Scale bars, 100 μm. *D*: Quantification of DHE fluorescence image of *C*. *P < 0.05 and ***P < 0.001 vs. LDLr$^{-/-}$ mice; ##P < 0.01 and ###P < 0.001 vs. LDLr$^{-/-}$Nrf2$^{-/-}$ mice. n = 5–7. *E*: Representative VCAM-1 and ICAM-1 immunostaining of aortic arch section (with arrows). Scale bars, 100 μm. mRNA levels of VCAM-1 (*F*) and ICAM-1 (*G*) in the aorta of LDLr$^{-/-}$Nrf2$^{-/-}$, STZ+HFD, and STZ+HFD+GYY4137 mice (n = 5). *H*: mRNA levels of HO-1 in the aorta (n = 5). Data shown are mean ± SEM. *P < 0.05 and **P < 0.01 vs. control.

on activation of the Nrf2 pathway, EA.hy926 cells were transfected with Nrf2 siRNA for 24 h before H_2S and HG+ox-LDL treatment. Western blotting revealed that individual transfection with Nrf2 siRNA successfully reduced Nrf2 protein expression at 24 h posttransfection, as compared with negative control siRNA-transfected (Ctl siRNA) cells (Fig. 7*A*). Nrf2 knockdown abrogated H_2S-mediated suppression of ROS production induced by HG+ox-LDL in endothelial cells (Fig. 7*B* and *C*). Furthermore, inhibition of HO-1 expression or activity by

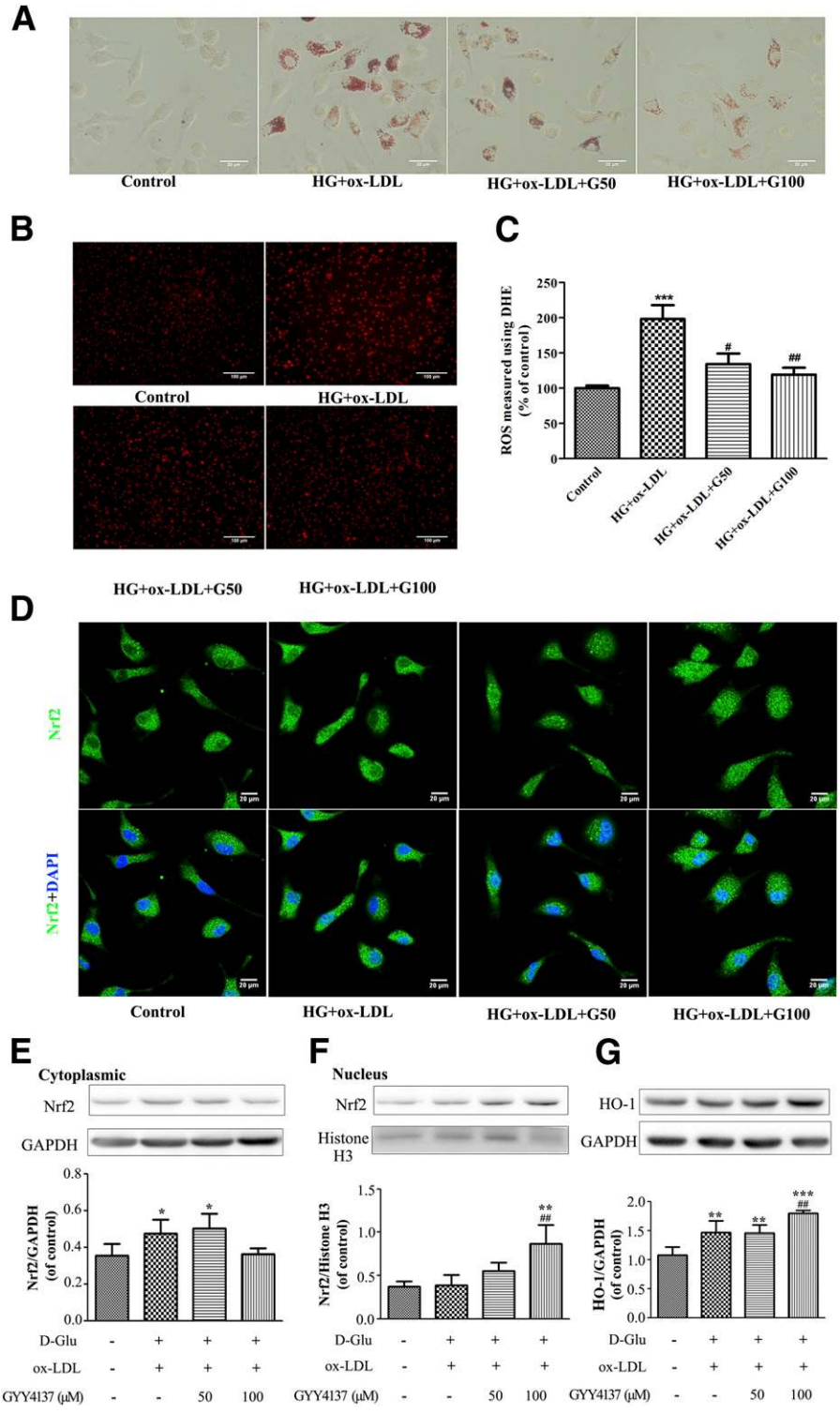

Figure 4—Effects of H_2S on HG+ox-LDL-treated primary peritoneal macrophages. Isolated peritoneal macrophages from C57BL/6 mice were treated with D-glucose (D-Glu) (25 mmol/L) plus ox-LDL (50 mg/L) in the presence or absence of GYY4137 (50 or 100 μmol/L) for 24 h. *A*: Macrophages incubated as above and stained with ORO. Scale bars, 20 μm. *B*: Representative DHE-stained images showing ROS generation in each condition. Scale bars, 50 μm. *C*: Quantification of DHE fluorescence image of *B*. ***$P < 0.01$ vs. untreated control; #$P < 0.05$ and ##$P < 0.01$ vs. treatment with HG+ox-LDL. $n = 5$. *D*: Immunohistochemistry was performed on macrophages stained with antibody directed against Nrf2 (green) and DAPI (blue). Scale bars, 20 μm. Western blotting analysis and quantification of cytoplasmic (*E*) and nuclear (*F*) Nrf2 protein. GAPDH and histone H3 were used for normalization for cytoplasmic and nuclear proteins, respectively ($n = 4$). *G*: Western blotting analysis and quantification of HO-1 protein expression ($n = 4$). Data shown are mean ± SEM. *$P < 0.05$, **$P < 0.01$, and ***$P < 0.001$ vs. untreated control; ##$P < 0.01$ vs. treatment with HG+ox-LDL.

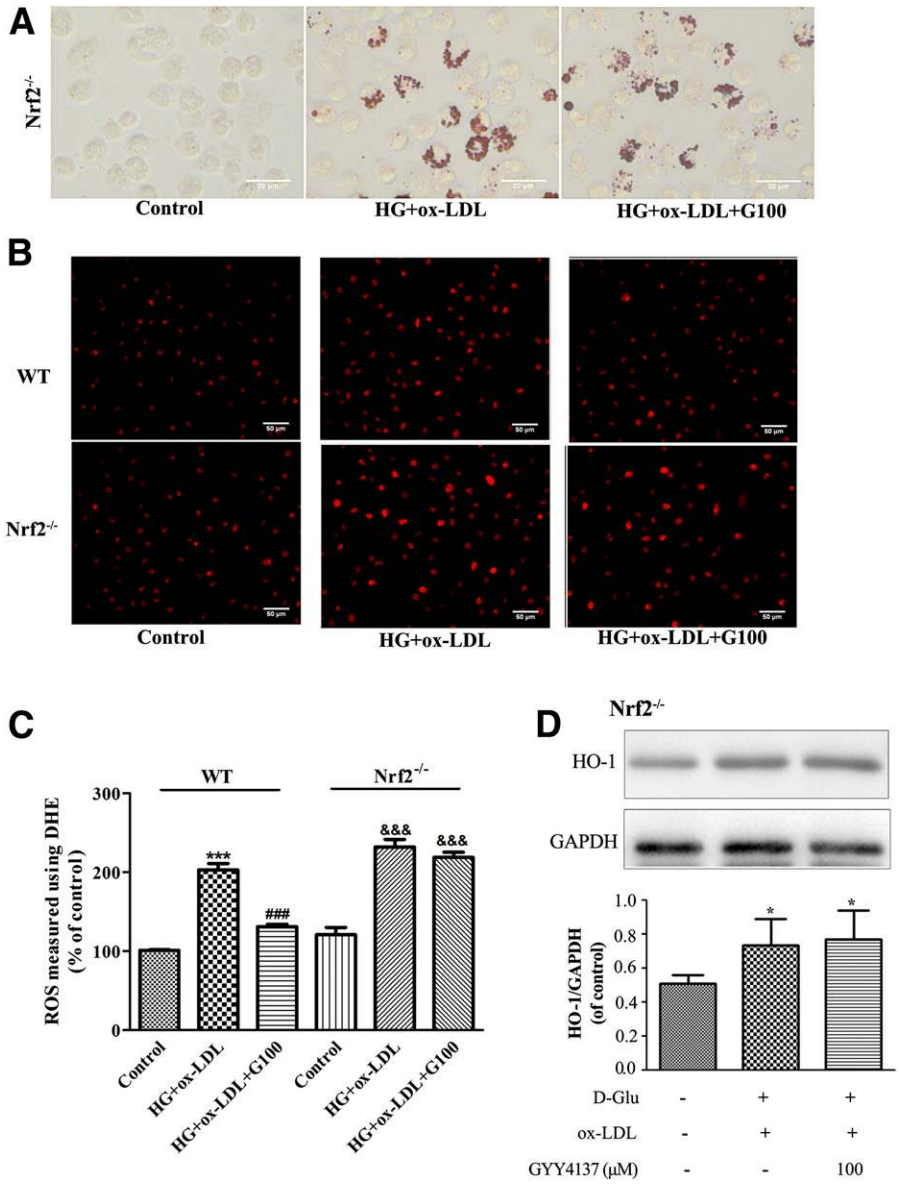

Figure 5—Effects of H_2S on HG+ox-LDL–treated primary peritoneal macrophages from Nrf2$^{-/-}$ mice. Isolated peritoneal macrophages from C57BL/6 (WT) and Nrf2$^{-/-}$ mice were treated with D-glucose (D-Glu) (25 mmol/L) plus ox-LDL (50 mg/L) in the presence or absence of GYY4137 (100 μmol/L) for 24 h. *A*: Macrophages from Nrf2$^{-/-}$ mice were stained with ORO. Scale bars, 20 μm. *B*: Representative DHE-stained images of macrophages from WT and Nrf2$^{-/-}$ mice. Scale bars, 50 μm. *C*: Quantification of DHE fluorescence image of *B*. ***P < 0.001 vs. WT control; ###P < 0.001 vs. WT with HG+ox-LDL; &&&P < 0.001 vs. Nrf2$^{-/-}$ control. n = 3. *D*: Western blotting analysis and quantification of HO-1 protein expression in macrophages from Nrf2$^{-/-}$ mice (n = 4). Data shown are mean ± SEM. *P < 0.05 vs. untreated control.

siRNA or ZnPP abolished the protective effects of H_2S (Supplementary Fig. 10). Together, these results indicate that the antioxidative and anti-inflammatory effects of H_2S in the presence of HG+ox-LDL are partially mediated by the Nrf2/HO-1 pathway in endothelial cells.

H_2S S-sulfhydrylated Keap1 at Cys151 to Regulate Nrf2 Activity and Reduce ROS Generation in HG+ox-LDL–Treated Endothelial Cells

Generally, Nrf2 is retained in an unactivated state binding with Keap1 in the cytoplasm, which serves as an adaptor for the degradation of Nrf2. Nrf2 can be activated by physiological stimuli that disrupt Keap1-Nrf2 interactions leading to nuclear translocation of Nrf2 (22). To further explore the mechanisms of Nrf2 activation, we immunoprecipitated the cell lysate using an anti-Keap1 antibody and blotted for Nrf2. The results showed that GYY4137 decreased the Nrf2/Keap1 interaction in HG+ox-LDL–treated endothelial cells (Fig. 8*A*). S-sulfhydration, the addition of one sulfhydryl to the thiol side of the cysteine residue and formation of a persulfide group (R-S-S-H), has been identified as a novel

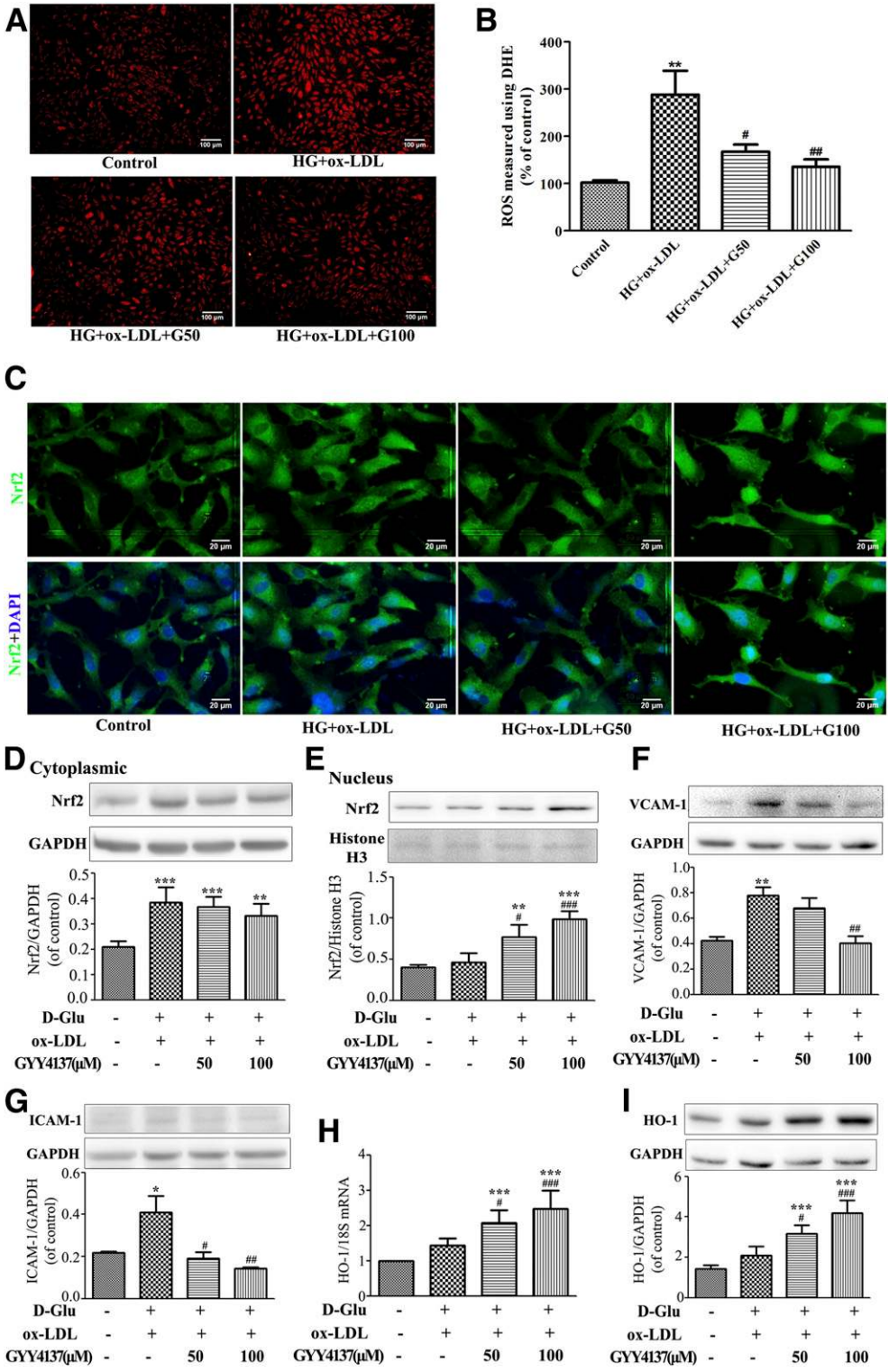

Figure 6—Effects of H_2S on HG+ox-LDL–treated endothelial cells. HUVECs were treated with D-glucose (D-Glu) (25 mmol/L) plus ox-LDL (50 mg/L) in the presence or absence of GYY4137 (50 or 100 μmol/L) for 24 h. *A*: Representative DHE-stained images showing ROS generation. Scale bars, 100 μm. *B*: Quantification of DHE fluorescence image of *A*. $^{**}P < 0.01$ vs. untreated control; $\#P < 0.05$ and $\#\#P < 0.01$ vs. treatment with HG+ox-LDL. $n = 5$. *C*: Immunohistochemistry was performed on HUVECs stained with antibody directed against Nrf2 (green) and DAPI (blue). Scale bars, 20 μm. Western blotting analysis and quantification of cytoplasmic (*D*) and nuclear (*E*) Nrf2 protein. GAPDH and histone H3 were used for normalization for cytoplasmic ($n = 5$) and nuclear ($n = 4$) proteins, respectively. Western blotting analysis and quantification of VCAM-1 (*F*) ($n = 4$) and ICAM-1 (*G*) ($n = 3$) protein. *H*: mRNA levels of HO-1 ($n = 5$). *I*: Western blotting analysis and quantification of HO-1 protein expression ($n = 4$). Data shown are mean ± SEM. $^{*}P < 0.05$, $^{**}P < 0.01$, and $^{***}P < 0.001$ vs. untreated control; $\#P < 0.05$, $\#\#P < 0.01$, and $\#\#\#P < 0.001$ vs. treatment with D-glucose plus ox-LDL.

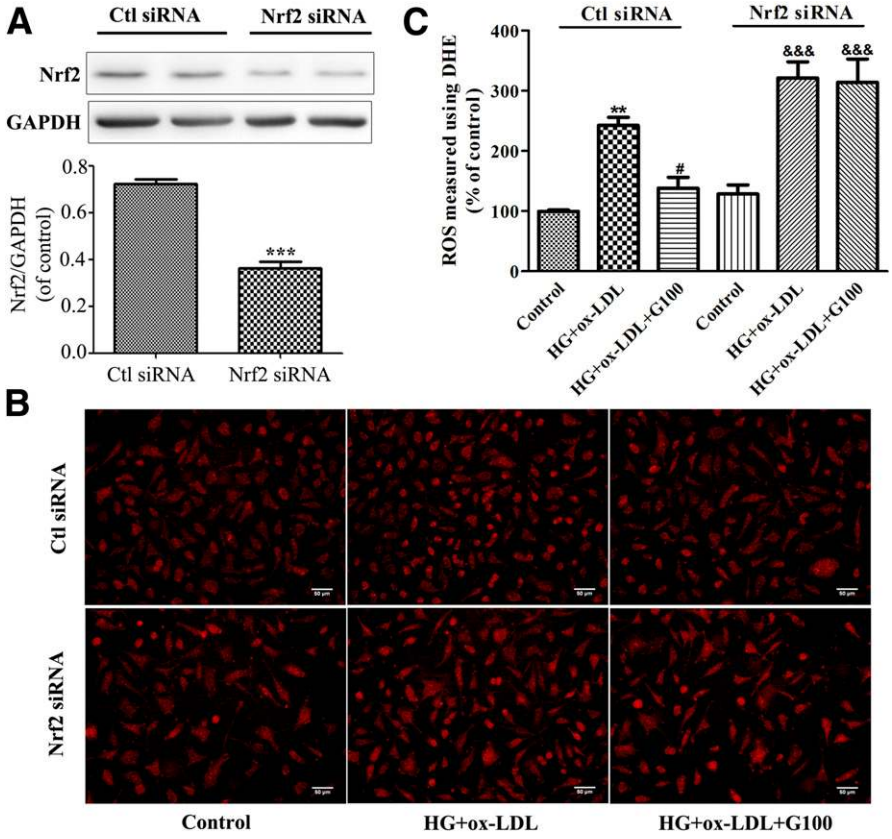

Figure 7—Effects of H_2S on HG+ox-LDL–treated Nrf2 knockdown endothelial cells. EA.hy926 endothelial cells were transfected with control siRNA (Ctl siRNA) or Nrf2 siRNA for 24 h and then treated with D-glucose (25 mmol/L) and ox-LDL (50 mg/L) in the presence or absence of GYY4137 (100 μmol/L) for 24 h. *A*: Western blotting analysis and quantification of Nrf2 ($n = 3$). Data shown are mean ± SEM. ***$P < 0.001$ vs. Ctl siRNA control. *B*: Representative DHE staining images. Scale bars, 50 μm. *C*: Quantification of DHE fluorescence image of *B*. **$P < 0.01$ vs. Ctl siRNA control; #$P < 0.05$ vs. Ctl siRNA with HG+ox-LDL; &&&$P < 0.001$ vs. Nrf2 siRNA control. $n = 5$.

posttranslational modification by H_2S in eukaryotic cells. However, the covalent modification in sulfhydration is reversed by reducing agents, such as dithiothreitol (23). We tested the S-sulfhydration of Nrf2 and found that H_2S donor GYY4137 or NaHS had no effect on Nrf2 S-sulfhydration (Supplementary Fig. 9*B*). We next investigated whether H_2S directly modified Keapl. After preincubation with GYY4137, EA.hy926 cells were treated with HG+ox-LDL and subjected to the "tag-switch" assay. There was stronger S-sulfhydration of Keap1 after GYY4137 incubation (Fig. 8*B*). To identify the S-sulfhydrated cysteine residue, Keap1 mutated at Cys151, Cys273, or Cys288 to alanine (C151A, C273A, or C288A) or wild type (WT) was transfected into endothelial cells. H_2S still enhanced S-sulfhydration on Keap1 after WT or mutated Keap1 at Cys288 but not at Cys151 and Cys273 overexpression (Fig. 8*C*). H_2S increased Nrf2 dissociation from Keap1 in HG+ox-LDL–treated endothelial cells after Keap1-WT and Keap1-C273A but not Keap1-C151A overexpression (Fig. 8*D*). Moreover, after Keap1 mutation at Cys151, H_2S failed to induce Nrf2 nuclear translocation or decrease the generation of superoxide (Fig. 8*E*–*G*). These findings indicate that S-sulfhydration of Cys151 in Keap1 is critical for Nrf2 activation in HG+ox-LDL–treated endothelial cells.

DISCUSSION

A complex interaction between inflammation, lipid deposition, monocytic infiltration, and endothelial dysfunction is responsible for the initiation and progression of diabetes-accelerated atherosclerosis (1). Experimental evidence for an antiatherosclerotic effect of H_2S has been obtained in numerous studies in hyperlipidemic animal and cell models (15,24–26), but the antiatherosclerotic effect in the context of diabetes has not been previously investigated. Recent data published by our group demonstrated that treatment with H_2S decreased aortic atherosclerotic plaque formation and partially restored aortic endothelium-dependent relaxation in $ApoE^{-/-}$ mice fed an HFD (15). Exogenous H_2S improved endothelium-dependent relaxation in isolated vascular rings incubated with HG and attenuated hyperglycemia-induced DNA injury and improved cellular viability in bEnd.3 microvascular endothelial cells (8). These data suggested that exogenous H_2S might serve as a treatment option for diabetes-associated atherosclerosis. Indeed, in the current study, we found that H_2S supplementation reduces lesion area and macrophage infiltration in diabetic $LDLr^{-/-}$ mice. In agreement with these findings, we

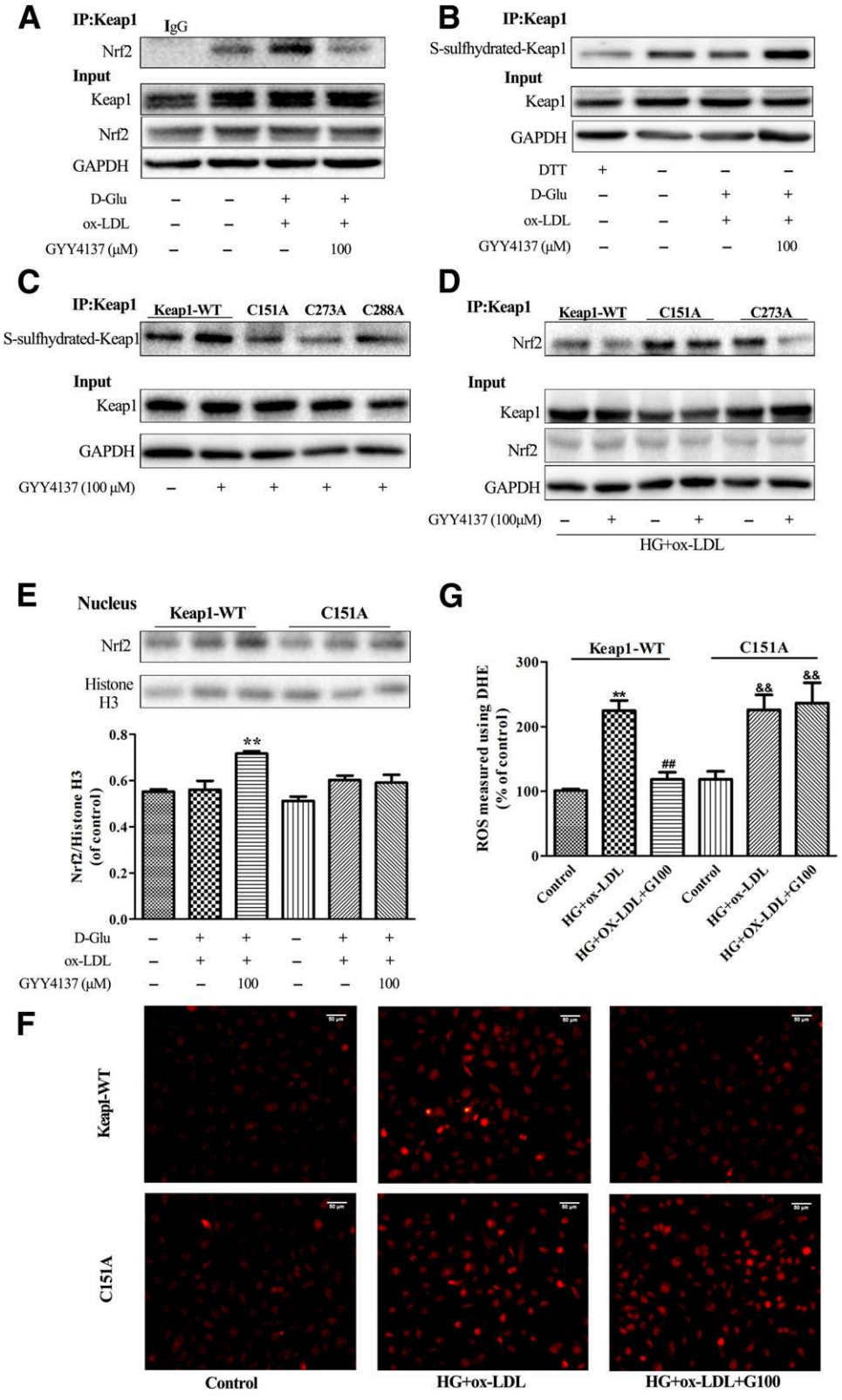

Figure 8— H_2S S-sulfhydrylated Keap1 at Cys151 to regulate Nrf2 transcription activity and reduce the generation of ROS in HG+ox-LDL–treated endothelial cells. *A*: EA.hy926 endothelial cells were treated with GYY4137 (100 μmol/L) followed by D-glucose (D-Glu) (25 mmol/L) plus ox-LDL (50 mg/L) stimulation for 24 h. Cell lysates were immunoprecipitated with an anti-Keap1 or an anti-IgG antibody (negative control) and blotted with an anti-Nrf2 antibody (top panel). An aliquot of total lysate was analyzed for Keap1, Nrf2, and GAPDH expression (bottom panel). *B*: EA.hy926 endothelial cells were treated with dithiothreitol (DTT) (1 mmol/L, negative control) or D-glucose (25 mmol/L) plus ox-LDL (50 mg/L) in the presence or absence of GYY4137 (100 μmol/L) for 2 h. S-sulfhydration on Keap1 was detected with the "tag-switch" method. *C*: After plasmid transfection of Keap1-WT or mutated Keap1 at Cys151, Cys273, and Cys288 for 24 h followed by

also observed that H_2S treatment attenuated HG+ox-LDL–induced foam cell formation. Our study provides the first evidence that H_2S may prevent the development of diabetes-accelerated atherosclerosis, which is not related to any effects on circulating blood glucose or cholesterol.

Several pathological mechanisms have been proposed for diabetic vascular complications, including diabetes-accelerated atherosclerosis, such as increased polyol pathway flux, increased advanced glycation end product formation, and activation of protein kinase C, all of these in association with hyperglycemia-induced ROS accumulation (27). Endothelial cells and macrophages are both sources of ROS. Indeed, in our study, we demonstrated that STZ-treated $LDLr^{-/-}$ mice fed an HFD showed an increase in atherosclerotic plaques compared with nondiabetic $LDLr^{-/-}$ mice, accompanied by increased superoxide production in aorta, and this was further confirmed in HG+ox-LDL–treated macrophages and endothelial cells. The increase in ROS promotes the recruitment and accumulation of inflammatory cells to the developing atherosclerotic lesion. H_2S has also been shown to have powerful antioxidant properties. Exogenous H_2S attenuates the hyperglycemia-induced enhancement of ROS formation in endothelial cells and human U937 monocytes (8,28). In line with these findings, we observed that H_2S decreased superoxide generation in macrophages and endothelial cells cultured with HG+ox-LDL. Furthermore, we showed that superoxide production in the aortas of diabetic $LDLr^{-/-}$ mice was reduced after H_2S administration. In this study, we show for the first time that inhibition of HG+ox-LDL–generated ROS with H_2S prevents the diabetes-induced increase in plaque area. Additionally, we found that H_2S attenuates the increase in aortic VCAM-1 and ICAM-1 expression.

Recent studies indicate that H_2S may upregulate endogenous antioxidants through an Nrf2-dependent signaling pathway (12) to combat oxidative stress. To date, the role of Nrf2 in atherosclerosis remains controversial. Myeloid Nrf2 deficiency aggravates both early and late stages of atherosclerosis in $LDLr^{-/-}$ mice (29,30). Ellagic acid improves oxidant-induced endothelial dysfunction and atherosclerosis partly via Nrf2 activation (31). In contrast to these reported protective actions, Nrf2 has also been ascribed as having potentially proatherogenic functions, in that $ApoE^{-/-}Nrf2^{-/-}$ double KO mice exhibited reduced plaque (32). In diabetes-associated atherosclerosis, a novel analog of the Nrf2 agonist bardoxolone methyl has been found to reduce atherosclerotic lesions as well as oxidative stress and the proinflammatory mediators ICAM-1 and VCAM-1 in STZ-induced diabetic $ApoE^{-/-}$ mice (7). Our data support previous findings regarding the protective actions of Nrf2 and suggest that H_2S can attenuate endothelial dysfunction, foam cell formation, and atherosclerosis in the context of diabetes, at least partially via the Nrf2/HO-1 pathway.

A widely accepted model for Nrf2 nuclear accumulation describes that a modification of the Keap1 cysteines leads directly to the dissociation of the Keap1-Nrf2 complex (33). Recently, one study suggested that Keap1 can be S-sulfhydrated at Cys151, which stimulates the dissociation of Nrf2 to enable its translocation to the nucleus (34). We found that Keap1 could be S-sulfhydrated at Cys151 and Cys273 simultaneously, but only the S-sulfhydration of Cys151 was involved in activation of Nrf2, which decreased the ROS generation to improve endothelial function. Kim et al. (35) found that thiol modification of Keap1 Cys288 is responsible for diallyl trisulfide–induced activation of Nrf2 signaling. However, in our study, Cys288 of Keap1 could not be S-sulfhydrated after treatment with GYY4137. This discrepancy may be attributed to different regulatory mechanisms in different cell types, the use of different H_2S treatment regiments giving rise to different kinetics of H_2S release. Nevertheless, this study demonstrates a significant role of Keap1 Cys151 S-sulfhydration in the protective effects of H_2S against diabetes-accelerated atherosclerosis.

In summary, our study provided definitive evidence that H_2S can lessen diabetes-accelerated atherosclerosis in $LDLr^{-/-}$ mice and improve hyperglycemia/ox-LDL–induced injury in macrophages and endothelial cells. This protective effect of H_2S can partly be attributed to activation of Nrf2 via Keap1 S-sulfhydration at Cys151. Our findings suggest that activation of Nrf2 may be a potential novel therapeutic strategy against diabetes-associated vascular disease and that exogenous H_2S administration in the form of an H_2S donor (GYY4137) may be of therapeutic benefit in the setting of diabetes-associated atherosclerosis. Finally, our study provides new insight into the mechanisms responsible for

GYY4137 (100 μmol/L) treated for another 2 h, S-sulfhydration on Keap1 was detected with the "tag-switch" method. *D*: Transfected cells were treated with D-glucose (25 mmol/L) plus ox-LDL (50 mg/L) in the presence or absence of GYY4137 (100 μmol/L) for another 24 h, cell lysates were immunoprecipitated with an anti-Keap1 antibody, and the immunoprecipitated proteins were subjected to immunoblot analysis with anti-Nrf2 antibodies (top panel). The total lysates were analyzed with anti-Keap1, anti-Nrf2, and anti-GAPDH antibodies (bottom panel). *E* and *F*: Transfected cells were treated with D-glucose (25 mmol/L) plus ox-LDL (50 mg/L) in the presence or absence of GYY4137 (100 μmol/L) for 24 h. Nuclear extracts prepared from cells were subjected to Western blotting analysis for detecting the nuclear localization of Nrf2 ($n = 4$). ROS accumulation was determined by the DHE assay. Scale bars, 50 μm. Data shown are mean ± SEM. $^{**}P < 0.01$ vs. Keap1-WT–transfected cells treated with D-glucose plus ox-LDL. *G*: Quantification of DHE fluorescence image of *F*. $^{**}P < 0.01$ vs. untreated Keap1-WT–transfected cells; $\#\#P < 0.01$ vs. Keap1-WT–transfected cells treated with D-glucose and ox-LDL; $\&\&P < 0.01$ vs. untreated C151A-transfected cells. $n = 4$.

the antiatherosclerotic effects of H_2S in the context of diabetes.

Acknowledgments. The authors thank Hongliang Li (Renmin Hospital of Wuhan University) for providing the $Nrf2^{-/-}$ mice.

Funding. This work was supported by grants from the National Natural Science Foundation of China (81200197, 81170083, and 81330004) and the National Basic Research Program of China 973 (2011CB503903 and 2012CB517803).

Duality of Interest. No potential conflicts of interest relevant to this article were reported.

Author Contributions. L.X. and Y.G. researched data, contributed to discussion, and edited the manuscript. M.W., S.Z., W.W., Y.M., Y.H., and Y.W. researched data. G.M. contributed to discussion and proofread the manuscript. G.L. designed the study and reviewed data. P.K.M., X.W., H.W., Z.Z., and Y.Y. reviewed the manuscript. A.F. contributed to discussion and rewrote the manuscript. Z.H. reviewed data and edited the manuscript. Y.J. designed the study, reviewed data, and edited the manuscript. All authors approved the final version of the manuscript. Y.J. is the guarantor of this work and, as such, had full access to all the data in the study and takes responsibility for the integrity of the data and the accuracy of the data analysis.

References

1. Eckel RH, Wassef M, Chait A, et al. Prevention Conference VI: Diabetes and Cardiovascular Disease: Writing Group II: pathogenesis of atherosclerosis in diabetes. Circulation 2002;105:e138–e143
2. Forbes JM, Cooper ME. Mechanisms of diabetic complications. Physiol Rev 2013;93:137–188
3. Ma Q. Role of nrf2 in oxidative stress and toxicity. Annu Rev Pharmacol Toxicol 2013;53:401–426
4. Niture SK, Khatri R, Jaiswal AK. Regulation of Nrf2-an update. Free Radic Biol Med 2014;66:36–44
5. Xu X, Luo P, Wang Y, Cui Y, Miao L. Nuclear factor (erythroid-derived 2)-like 2 (NFE2L2) is a novel therapeutic target for diabetic complications. J Int Med Res 2013;41:13–19
6. Ramprasath T, Selvam GS. Potential impact of genetic variants in Nrf2 regulated antioxidant genes and risk prediction of diabetes and associated cardiac complications. Curr Med Chem 2013;20:4680–4693
7. Tan SM, Sharma A, Stefanovic N, et al. Derivative of bardoxolone methyl, dh404, in an inverse dose-dependent manner lessens diabetes-associated atherosclerosis and improves diabetic kidney disease. Diabetes 2014;63:3091–3103
8. Suzuki K, Olah G, Modis K, et al. Hydrogen sulfide replacement therapy protects the vascular endothelium in hyperglycemia by preserving mitochondrial function. Proc Natl Acad Sci U S A 2011;108:13829–13834
9. Zhou X, Feng Y, Zhan Z, Chen J. Hydrogen sulfide alleviates diabetic nephropathy in a streptozotocin-induced diabetic rat model. J Biol Chem 2014;289:28827–28834
10. Si YF, Wang J, Guan J, Zhou L, Sheng Y, Zhao J. Treatment with hydrogen sulfide alleviates streptozotocin-induced diabetic retinopathy in rats. Br J Pharmacol 2013;169:619–631
11. Zhou X, An G, Lu X. Hydrogen sulfide attenuates the development of diabetic cardiomyopathy. Clin Sci (Lond) 2015;128:325–335
12. Calvert JW, Jha S, Gundewar S, et al. Hydrogen sulfide mediates cardioprotection through Nrf2 signaling. Circ Res 2009;105:365–374
13. Peake BF, Nicholson CK, Lambert JP, et al. Hydrogen sulfide preconditions the db/db diabetic mouse heart against ischemia-reperfusion injury by activating Nrf2 signaling in an Erk-dependent manner. Am J Physiol Heart Circ Physiol 2013;304:H1215–H1224
14. Zhou X, An G, Chen J. Inhibitory effects of hydrogen sulphide on pulmonary fibrosis in smoking rats via attenuation of oxidative stress and inflammation. J Cell Mol Med 2014;18:1098–1103
15. Liu Z, Han Y, Li L, et al. The hydrogen sulfide donor, GYY4137, exhibits anti-atherosclerotic activity in high fat fed apolipoprotein E(-/-) mice. Br J Pharmacol 2013;169:1795–1809
16. Cheng WL, Wang PX, Wang T, et al. Regulator of G-protein signalling 5 protects against atherosclerosis in apolipoprotein E-deficient mice. Br J Pharmacol 2015;172:5676–5689
17. Mauldin JP, Srinivasan S, Mulya A, et al. Reduction in ABCG1 in type 2 diabetic mice increases macrophage foam cell formation. J Biol Chem 2006;281:21216–21224
18. Ferro A, Queen LR, Priest RM, et al. Activation of nitric oxide synthase by beta 2-adrenoceptors in human umbilical vein endothelium in vitro. Br J Pharmacol 1999;126:1872–1880
19. Xie L, Liu Z, Lu H, et al. Pyridoxine inhibits endothelial NOS uncoupling induced by oxidized low-density lipoprotein via the PKCα signalling pathway in human umbilical vein endothelial cells. Br J Pharmacol 2012;165:754–764
20. Mi Q, Chen N, Shaifta Y, et al. Activation of endothelial nitric oxide synthase is dependent on its interaction with globular actin in human umbilical vein endothelial cells. J Mol Cell Cardiol 2011;51:419–427
21. Park CM, Macinkovic I, Filipovic MR, Xian M. Use of the "tag-switch" method for the detection of protein S-sulfhydration. Methods Enzymol 2015;555:39–56
22. Zhang DD, Lo SC, Sun Z, Habib GM, Lieberman MW, Hannink M. Ubiquitination of Keap1, a BTB-Kelch substrate adaptor protein for Cul3, targets Keap1 for degradation by a proteasome-independent pathway. J Biol Chem 2005;280:30091–30099
23. Mustafa AK, Gadalla MM, Sen N, et al. H2S signals through protein S-sulfhydration. Sci Signal 2009;2:ra72
24. Mani S, Li H, Untereiner A, et al. Decreased endogenous production of hydrogen sulfide accelerates atherosclerosis. Circulation 2013;127:2523–2534
25. Wang XH, Wang F, You SJ, et al. Dysregulation of cystathionine γ-lyase (CSE)/hydrogen sulfide pathway contributes to ox-LDL-induced inflammation in macrophage. Cell Signal 2013;25:2255–2262
26. Wang Y, Zhao X, Jin H, et al. Role of hydrogen sulfide in the development of atherosclerotic lesions in apolipoprotein E knockout mice. Arterioscler Thromb Vasc Biol 2009;29:173–179
27. Brownlee M. Biochemistry and molecular cell biology of diabetic complications. Nature 2001;414:813–820
28. Manna P, Jain SK. L-cysteine and hydrogen sulfide increase PIP3 and AMPK/PPARγ expression and decrease ROS and vascular inflammation markers in high glucose treated human U937 monocytes. J Cell Biochem 2013;114:2334–2345
29. Collins AR, Gupte AA, Ji R, et al. Myeloid deletion of nuclear factor erythroid 2-related factor 2 increases atherosclerosis and liver injury. Arterioscler Thromb Vasc Biol 2012;32:2839–2846
30. Ruotsalainen AK, Inkala M, Partanen ME, et al. The absence of macrophage Nrf2 promotes early atherogenesis. Cardiovasc Res 2013;98:107–115
31. Ding Y, Zhang B, Zhou K, et al. Dietary ellagic acid improves oxidant-induced endothelial dysfunction and atherosclerosis: role of Nrf2 activation. Int J Cardiol 2014;175:508–514
32. Barajas B, Che N, Yin F, et al. NF-E2-related factor 2 promotes atherosclerosis by effects on plasma lipoproteins and cholesterol transport that overshadow antioxidant protection. Arterioscler Thromb Vasc Biol 2011;31:58–66
33. Holland R, Fishbein JC. Chemistry of the cysteine sensors in Kelch-like ECH-associated protein 1. Antioxid Redox Signal 2010;13:1749–1761
34. Yang G, Zhao K, Ju Y, et al. Hydrogen sulfide protects against cellular senescence via S-sulfhydration of Keap1 and activation of Nrf2. Antioxid Redox Signal 2013;18:1906–1919
35. Kim S, Lee HG, Park SA, et al. Keap1 cysteine 288 as a potential target for diallyl trisulfide-induced Nrf2 activation. PLoS One 2014;9:e85984